(Continued from page 954)

Substrate-Inhibited Kinetics With Catalyst Deactivation in an Isothermal CSTR

DUONG D. DO

Dept. of Chemical Engineering
California Institute of Technology
Pasadena, CA 91125

and

RALPH H. WEILAND

Dept. of Chemical Engineering
Clarkson College of Technology
Potsdam, NY 13676

II. Multiple Pseudosteady States and Reactor Failure

Analytical expressions are derived for the time and magnitude of failure of an isothermal CSTR with substrate-inhibited kinetics, caused by slow catalyst deactivation under three types of parallel and series mechanisms. Reactors operating at high space velocity are found to be most susceptible to early failure and poisoning by product is more dangerous than by reactant. The magnitude of the jump across steady states depends solely on the Langmuir-Hinshelwood kinetic parameters and a detailed analysis of reactor behavior during the jump itself is given.

SCOPE

Reactions which exhibit so-called abnormal kinetics are typified by those with Langmuir-Hinshelwood or substrate inhibited rate expressions. Such systems offer the possibility of a reactor operating at one of a multiplicity of steady states even under isothermal conditions. When the catalyst is also being slowly deactivated, one may find that a reactor which has been operating satisfactorily suddenly ceases to function or begins performing at a much lower conversion. Our purpose in this work is to determine the time of failure of a CSTR from basic physico-chemical data and to give a detailed description of the way in which reactor performance moves from one (acceptable) steady state to another (unsatisfactory) one, for substrate or Langmuir-Hinshelwood kinetics, accompanied by catalyst poisoning.

We have shown previously (Do and Weiland, 1980a) that for enzyme-catalyzed reactions, the forms of rate expression for the main reaction and the deactivation process must bear certain minimum relationships. Such self-consistent rate forms are used here. The effect of both reactant and product poisoning is considered and three mechanisms are examined for each case.

The performance of an isothermal CSTR with catalytic reactions of normal kinetic form and with simultaneous catalyst deactivation has been analyzed by Do and Weiland (1979a, 1979b) using the techniques of singular perturbation theory. In a precursory study, we reported the results of a similar analysis for substrate inhibition at a unique steady state (Do and Weiland, 1980b). There the periods corresponding to reactor startup and serious catalyst deactivation were analyzed using separate asymptotic expansions. These were then matched to give a complete description of reactor performance from startup to shutdown.

For substrate-inhibited kinetics with catalyst deactivation, these simple solution procedures fail when multiple steady states exist because of a sudden jump from one quasisteady state to another resulting from the catalyst decaying and passing through some critical level of activity. Singular perturbation methods are still applicable, but the behavior around the time of the jump requires a separate and more detailed analysis. In addition to the method of matched asymptotic expansions, we bring certain results of bifurcation theory to bear on the problem in an effort to find not only the jump time but also the way in which the reactor moves from one quasisteady state to another.

CONCLUSIONS AND SIGNIFICANCE

The sudden and spectacular failure of an isothermal CSTR which is caused by slow catalyst deactivation in systems with substrate-inhibited kinetics is analyzed. For three types of parallel and series poisoning mechanisms, it is found that at some stage the reactor will quickly jump from one pseudosteady state to another. At this second steady state, reactor conversion may be very low, despite the fact that the catalyst still retains a large proportion of its initial activity.

Analytical expressions are derived for the time of failure from startup and the magnitude of the failure, or change in

Correspondence concerning this paper should be addressed to R. H. Weiland.

Part I of this paper appears on page 948 of this issue.

0001-1541-80-4189-1020-$01.15.

operation, which results. It is found that reactors operating at high space velocities are most subject to early failure and that poisoning by the product of reaction can cause failure many hundreds of times earlier in reactor operation than is the case for reactant poisoning.

The magnitude of the sudden drop in conversion is independent of the space velocity through the reactor, of the poisoning type, and of the details of the poisoning mechanism. It is found to depend solely on the values of the kinetic parameters in the Langmuir-Hinshelwood rate expressions.

The analysis also provides a detailed description of the performance of the reactor during the brief time it takes to move between steady states. This passage through criticality is characterized by two distinct time scales. One of them corresponds to a time made nondimensional on the space velocity or rate constant for the main reaction; the other is a much longer time and has to do with the nondimensional rate constant for deactivation raised to a fractional power. Thus, the two quasi-steady states are made continuous across the jump by matching with two separate solutions valid during the jump. The net result is a description of reactor performance which is continuous and smooth throughout all time, even during the transition from one steady state to the other.

This paper does not allow for either external or internal (pore) diffusional resistances. This is probably of little consequence for conventional catalysis over metal surfaces; for immobilized enzymes, pore diffusion would affect the results.

INTRODUCTION

In a precursory study (Do and Weiland, 1980b), the effect of reactant- and product-induced catalyst deactivation on the performance of an isothermal CSTR with a unique pseudosteady state and Langmuir-Hinshelwood kinetics was analyzed. The assumption that deactivation took place at a much slower rate than the main reaction allowed the method of matched asymptotic expansions to be applied in a straightforward way. The result was a simple analytical description of reactor performance and catalyst activity, valid over the entire period from reactor start-up to final loss of activity. The usual assumption of an initial steady state did not have to be made separately.

In the current work, we are interested in the behavior of the same reactor when it is operating in that region of parameter space which admits of multiple steady states. Conditions for the uniqueness of these steady states have recently been developed by De Vera and Varma (1979) for a substrate-inhibited (Langmuir-Hinshelwood) enzyme reaction in a tubular reactor, in the absence of simultaneous enzyme deactivation. Multiplicity and stability in enzyme systems have been discussed by Bruns et al. (1973).

When a multiplicity of steady states is coupled with a slowly deactivating catalyst, some rather exotic phenomena can be anticipated. For systems which possess at least two stable steady states, the reactor may suddenly jump from one steady state to another, as the catalyst decays in activity. When this occurs, a reactor which was operating at high conversion may suddenly be found to be incapable of virtually any reaction at all, despite the fact that the catalyst is still quite active. It would be useful to be able to predict the time at which loss of performance will occur.

Deactivating systems are inherently time-dependent so that true steady states are replaced by pseudosteady ones at any particular level of activity. The study of multiplicity and stability of pseudosteady states is analogous to similar studies in non-decaying systems, but now using the pseudosteady equations. (This implicitly assumes that catalyst deactivation is a slow process compared to other reaction rates). For substrate inhibited kinetics with a deactivating catalyst, at most three quasisteady states can be found in a CSTR operated isothermally, but not all of them are stable. Gavalas (1968) has used topological arguments to show that out of $(2m + 1)$ possibilities, at least m are unstable, except under special circumstances. In the present problem we will show that only the middle pseudosteady state is globally unstable.

When there are multiple steady states the direct application of matched asymptotic expansions in the startup and deactivating periods breaks down because the outer, or long time, solution possesses two separate branches. At some stage which we call the branching time, the outer solution jumps discontinuously from one quasisteady state to the other.

The case of two stable quasisteady states is shown in Figure 1, where it can be seen that the concentration of reactant, A, rises smoothly from a pseudosteady level A^+, achieved shortly after startup, to a value A_*. But because the catalyst slowly continues to be deactivated, the slope of the line marked $H(1-A)/a$ becomes increasingly negative and operation at A_* ceases to be possible. The reactant concentration must suddenly rise to a new value A^* in a very short time. This corresponds to a jump in the solution from the *lower branch* in which $A^+ < A < A_*$ to an *upper branch where* $A > A^*$. The catalyst activity does not experience a sudden change because the rate of deactivation is always slow. Thus, when the reactant concentration reaches A^*, reactor conversion suddenly drops to a low level despite the fact that the catalyst may still be relatively active.

The upper and lower branches are connected through a *branching inner solution*, valid within a thin layer about the branching time and of thickness determined largely by the space velocity in the reactor. As will be shown in a subsequent section,

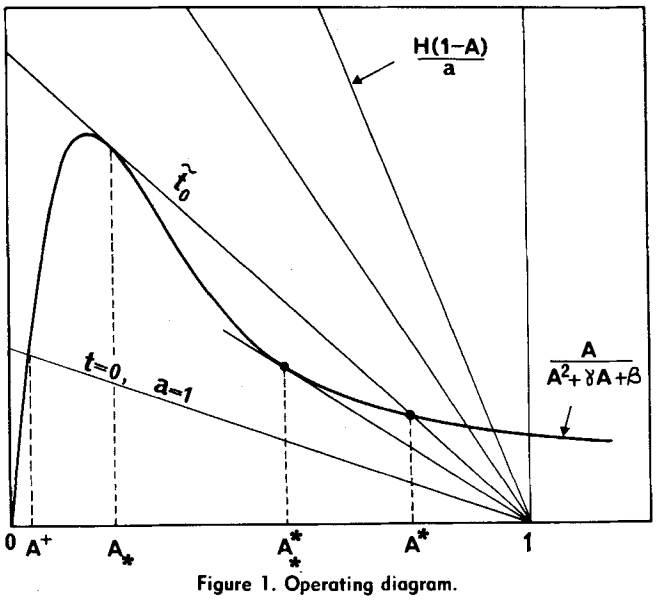

Figure 1. Operating diagram.

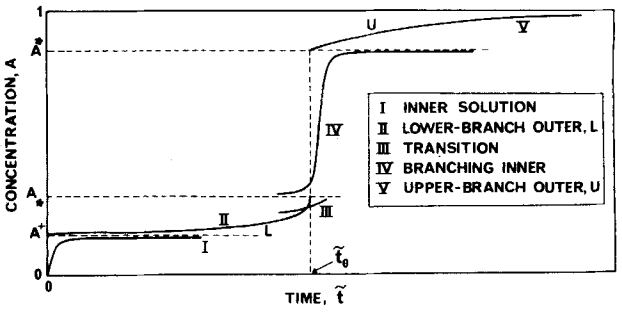

Figure 2. Schematic of time-dependence of reactant concentration.

this branching inner solution can be matched successfully with the upper branch of the outer solution (*where* $A > A^*$) but fails to match with the lower branch. This failure is due to the existence of a distinguished (singular) limit which necessitates the analysis of *another* transition region across which the lower-branch outer solution can be matched with the branching inner solution. The net result is that the concentration of reactant A will be described as a *continuous* function of time even across the jump. The situation is depicted in Figure 2, where it can be seen that the five solutions: I, inner; II, lower-branch outer; III, transition; IV, branching inner; and V, upper-branch outer are all required to be determined and matched for a complete description of reactor performance.

SYSTEM EQUATIONS

For a substrate-inhibited reaction occurring in a well-mixed, isothermal CSTR without mass transfer resistances the nondimensional transient mass balance equations for reactant and product, respectively, are:

$$\dot{A} = H(1 - A) - Aa/(A^2 + \gamma A + \beta), \tag{1a}$$

$$\dot{B} = -HB + Aa/(A^2 + \gamma A + \beta), \tag{1b}$$

The feed to the reactor has been assumed product-free (Do and Weiland, 1980b). Rate expressions for catalyst activity which are consistent with Langmuir-Hinshelwood kinetics for the main reaction have been shown previously (Do and Weiland, 1980a) to have the form:

$$\dot{a} = \begin{cases} -\epsilon A^n a/(A^2 + \gamma A + \beta), & \text{(1c)} \\ -\epsilon A^{n-1} B a/(A^2 + \gamma A + \beta), & \text{(1d)} \end{cases}$$

for parallel and series poisoning, respectively. The various integer values which n may assume correspond to different deactivation mechanisms as discussed by Do and Weiland (1980b). The parameter H is a nondimensional space velocity and ϵ is the ratio of the rate of deactivation to that of the main reaction; we will assume $\epsilon << 1$. Time has been scaled on the reaction rate constant.

Prior to reactor startup, the catalyst has unit activity and only inert material is present in the fluid.

$$A(0) = B(0) = 0, \tag{1e}$$

$$a(0) = 1 \tag{1f}$$

At reactor startup, a product-free feed having unit nondimensional reactant concentration is introduced at a constant flow rate. Our objective is a long-time description of reactor performance.

The case of series deactivation (Eq. 1d) can be reduced to a set of equations in terms of only A and a as outlined previously (Do and Weiland, 1980b). Here, we will restrict our attention to a detailed analysis of parallel deactivation in which the reactant is directly responsible for the poisoning process ($n = 1$). The relevant equations describing the reactor are

$$\frac{dA}{dt} = H(1-a) - \frac{Aa}{A^2 + \gamma A + \beta} \overset{\text{def}}{=} g(A, a), \tag{2a}$$

$$\frac{da}{dt} = -\epsilon \frac{Aa}{A^2 + \gamma A + \beta}, \tag{2b}$$

with initial conditions

$$A(0) = 1, \tag{2c}$$

$$a(0) = 0 \tag{2d}$$

In the interests of space, the important results for $n = 1,2,3$ and both parallel and series deactivation will only be presented in tabular form—the analysis parallels that given here.

INNER SOLUTION

We exploit the fact that ϵ is a small parameter and expand the dependent variables in the series forms:

$$A(t;\epsilon) \sim A_o(t) + \epsilon A_1(t) + \ldots, \tag{3a}$$

$$a(t;\epsilon) \sim a_o(t) + \epsilon a_1(t) + \ldots \tag{3b}$$

At order unity the system given by Eqs. 2a and 2b is just

$$\frac{dA_o}{dt} = H(1 - A_o) - A_o a_o/(A_o^2 + \gamma A_o + \beta), \tag{4a}$$

$$\frac{da_o}{dt} = 0 \tag{4b}$$

It is obvious that these equations describe the period of reactor startup, during which the catalyst activity remains essentially constant, at least to leading order in ϵ.

Solutions are:

$$a_o(t) \equiv 1, \tag{5a}$$

$$\frac{A^{+2} + \gamma A^+ + \beta}{(A^+ - A')(A^+ - A'')} \ln\left(\frac{A^+ - A}{A^+}\right) + \frac{A'^2 + \gamma A' + \beta}{(A' - A^+)(A' - A'')} \ln\left(\frac{A' - A}{A'}\right) + \frac{A''^2 + \gamma A'' + \beta}{(A'' - A^+)(A'' - A')} \ln\left(\frac{A'' - A}{A''}\right) = -Ht, \tag{5b}$$

where A^+ is the smallest root of

$$A^3 + (\gamma - 1)A^2 + (\beta + H^{-1} - \gamma)A - \beta = 0 \tag{5c}$$

and A', A'' are the two other roots. These inner solutions will act as initial conditions for the outer (long-time) solutions developed in the next section.

OUTER SOLUTION

The time scale appropriate to the description of catalyst deactivation is:

$$\tilde{t} = \epsilon t \tag{6}$$

With this slow time, the governing Eqs. 2a and 2b become:

$$\epsilon \frac{d\tilde{A}}{d\tilde{t}} = H(1 - \tilde{A}) - \frac{\tilde{A}\tilde{a}}{\tilde{A}^2 + \gamma\tilde{A} + \beta}, \tag{7a}$$

$$\frac{d\tilde{a}}{d\tilde{t}} = -\frac{\tilde{A}\tilde{a}}{\tilde{A}^2 + \gamma\tilde{A} + \beta} \tag{7b}$$

We seek a solution of the form:

$$\tilde{A}(\tilde{t};\epsilon) = \tilde{A}_o(\tilde{t}) + \epsilon\tilde{A}_1(\tilde{t}) + \ldots, \tag{8a}$$

$$\tilde{a}(\tilde{t};\epsilon) = \tilde{a}_o(\tilde{t}) + \epsilon\tilde{a}_1(\tilde{t}) + \ldots \tag{8b}$$

At order unity the equations are:

$$H(1 - \tilde{A}_o) - \frac{\tilde{A}_o\tilde{a}_o}{\tilde{A}_o^2 + \gamma\tilde{A}_o + \beta} = g(\tilde{A}_o, \tilde{a}_o) = 0, \tag{9a}$$

$$\frac{d\tilde{a}_o}{d\tilde{t}} = -\frac{\tilde{A}_o\tilde{a}_o}{\tilde{A}_o^2 + \gamma\tilde{A}_o + \beta}, \tag{9b}$$

$$\tilde{a}_o(0) = 1, \tag{9c}$$

$$\tilde{A}_o(0) = A^+ \tag{9d}$$

It is easy to show that Eq. 9d is the correct initial condition to guarantee automatic matching with the inner solution given by Eqs. 5a to 5c. Eqs. 9a to 9d possess the solution:

$$\tilde{a}_o = H(1 - \tilde{A}_o)(\tilde{A}_o^2 + \gamma\tilde{A}_o + \beta)/\tilde{A}_o, \tag{10a}$$

$$2(A^+ - \tilde{A}_o) - \beta\ln(\tilde{A}_o/A^+) + (1 + \beta + \gamma)\ln[(1 - A^+)/(1 - \tilde{A}_o)] + \beta(1/A^+ - 1/\tilde{A}_o) = \tilde{t} \tag{10b}$$

already matched with Eqs. 5a to 5c.

This outer solution breaks down in the vicinity of the concentration jump however, because there the term $d\tilde{A}_o/d\tilde{t}$ cannot be neglected. Indeed, on the time variable $\tilde{t}$, this derivative becomes infinite. Then the limit expansion process fails and the solution branches to another quasisteady state. Points at which the derivative $d\tilde{A}_o/d\tilde{t}$ is infinite are called *branch points*. The present system contains *two* branch points, namely, A_* and $A^\sharp$. Only the point A_* is relevant to the behavior of the reactor on the time variable $\tilde{t}$ because $A^\sharp$ lies in the transition region across which the lower and upper branches of the solution are connected. In terms of changes in $\tilde{A}$ with $\tilde{t}$, the point $A^\sharp$ is lost. But it is this point which is responsible for the need to connect the lower and upper branches through *two* transition expansions with different time scales.

Although $d\tilde{A}_o/d\tilde{t}$ is missing from Eqs. 9a to 9d, it can be recovered by differentiating and eliminating $\tilde{a}_o$ from these equations. This gives:

$$\frac{d\tilde{A}_o}{d\tilde{t}} = \frac{\tilde{A}_o^2(1-\tilde{A}_o)}{2\tilde{A}_o^3 + (\gamma-1)\tilde{A}_o^2 + \beta} \tag{11}$$

The derivative is infinite when

$$2\tilde{A}_o^3 + (\gamma-1)\tilde{A}_o^2 + \beta = 0 \tag{12}$$

Methods for cubic polynomials (Abramowitz and Stegun, 1970) indicate that a sufficient (but not necessary) condition for multiplicity is:

$$\gamma < 1 - 3\beta^{1/3} \tag{13}$$

If this inequality is satisfied there are three branch points, but only *two* of them, A_* and $A^\sharp$, correspond to positive A.

It is easy to prove that $(A_*, A^\sharp) \in (0, \frac{1}{2})$. Rearrange Eq. 12 as:

$$A^2 - 2A^3 = \beta + \gamma A^2 \tag{14}$$

The left-hand side is independent of the parameters β, γ and is only nonnegative for $A \in [0, \frac{1}{2}]$. But, the right-hand side is always positive. Thus, equality can be had only in Eq. 14 if $A \in (0, \frac{1}{2})$ for nonzero (β, γ).

The outer solution consists of the two segments L and U shown in Figure 2. The lower-branch outer solution is only valid for $\tilde{t} < \tilde{t}_o$, *where* $\tilde{t}_o$ is the branching time (corresponding strictly to A_*), while the upper-branch outer solution is valid for $\tilde{t} > \tilde{t}_o$. In L and U, the reactant concentration ranges over (A^+, A_*) and $(A^*, 1)$, respectively. Here A^* is the concentration to which the lower branch jumps; it corresponds to the start of the upper branch, in terms of the variable $\tilde{t}$. In the transition region, the concentration jumps from A_* to A^* in a very brief time; in so doing it passes through the second branch point $A^\sharp$ imbedded in that region.

The manner in which the outer solution jumps from the segments L to U can be demonstrated as follows; on linearizing the original Eq. 1a (in terms of the reaction time) about the outer solution $(\tilde{A}_o, \tilde{a}_o)$ we have:

$$\frac{d\omega}{dt} = \frac{\partial g(\tilde{A}_o, \tilde{a}_o)}{\partial \tilde{A}_o}\omega + 0(\omega^2) \tag{15}$$

in which $\omega = (A - \tilde{A}_o)$ is a deviation variable. The behavior of solutions to Eq. 15 is determined by the sign of the derivative, $\partial g/\partial A_o$, which we call an eigenvalue. As $t \to \infty$, we have asymptotic stability or instability accordingly as this eigenvalue is negative or positive, respectively.

The outer solution for A in the range (A^+, A_*) has negative eigenvalue and so it is stable. However, as A approaches A_* from below, the eigenvalue passes through zero and becomes positive for $A > A_*$; the solution becomes unstable. As A passes through the upper branch point $A^\sharp$, the eigenvalue again passes through zero and returns to negative values; the solution regains stability. Because $A^\sharp$ lies within the transition zone however, A quickly reaches a new quasisteady level A^* on a time scale given by the space velocity within the reactor. The time scale appropriate to the region $A_* < A < A^\sharp$ is a different matter and will be treated, when we come to a detailed consideration of the transition period.

The initial value of concentration, A^*, for the upper branch of the outer solution is a root of:

$$H(1-A) - Aa_*/(A^2 + \gamma A + \beta) = 0 \tag{16}$$

This equation possesses the double root:

$$A = A_* \tag{17}$$

and it can be shown that the third root can be given in terms of the first by:

$$A^* = \beta/A_*^2 \tag{18}$$

The lower branch outer solution is given by Eqs. 10a and 10b, while Eqs. 9a to 9d govern the upper branch with Eq. 18 acting as the initial condition. The solution is:

$$2(A^* - \tilde{A}_o) + \beta \ln\left(\frac{\tilde{A}_o}{A^*}\right) + (1+\beta+\gamma)\ln\left(\frac{1-A^*}{1-\tilde{A}_o}\right) + \beta\left(\frac{1}{A^*} - \frac{1}{\tilde{A}_o}\right) = \tilde{t} - \tilde{t}_o; \quad \tilde{t} > \tilde{t}_o \tag{19}$$

in which $\tilde{t}_o$ is the branching time, given by:

$$\tilde{t}_o = 2(A^+ - A_*) + \beta \ln\left(\frac{A_*}{A^+}\right) + (1+\beta+\gamma)\ln\left(\frac{1-A^+}{1-A_*}\right) + \beta\left(\frac{1}{A^+} - \frac{1}{A_*}\right) \tag{20}$$

The asymptotic behavior of the lower and upper branches as $\tilde{t} \to \tilde{t}_o$ is required for matching later on. We find that for $\tilde{t} \to \tilde{t}_{o-}$ from below,

$$\tilde{A}_o \sim A_* - \left[\frac{A_*(1-A_*)(\tilde{t}_o - \tilde{t})}{(\beta/A_*^2 - A_*)}\right]^{\frac{1}{2}}, \tag{21a}$$

while for $\tilde{t} \to \tilde{t}_{o+}$ from above,

$$\tilde{A}_o \sim A^* + \frac{A^{*2}(1-A^*)(\tilde{t} - \tilde{t}_o)}{2A^{*3} + (\gamma-1)A^{*2} + \beta} \tag{21b}$$

The two branches of the outer solution must now be joined.

Branching-Inner Solution

The thickness of the branching-inner region across which lower and upper branches of the outer solution join is determined by the space velocity in the reactor and not by the rate constant for deactivation. This suggests the rescaling of time according to:

$$\bar{t} = \frac{\tilde{t} - \tilde{t}_o - \delta(\epsilon)}{\epsilon} \tag{22}$$

Here, $\delta(\epsilon)$ represents a small time shift whose inclusion allows the matching of higher order terms in the asymptotic expansions. It is only found as a result of such matching (we will only consider the problem at leading order) but is included here to allow our results to be improved, if desired. Eqs. 9a and 9b become:

$$\frac{d\bar{A}}{d\bar{t}} = H(1-\bar{A}) - \frac{\bar{A}\bar{a}}{\bar{A}^2 + \gamma\bar{A} + \beta}, \tag{23a}$$

$$\frac{d\bar{a}}{d\bar{t}} = -\epsilon\frac{\bar{A}\bar{a}}{\bar{A}^2 + \gamma\bar{A} + \beta} \tag{23b}$$

Dependent variables are expanded in the asymptotic series:

$$\bar{A}(\bar{t};\epsilon) = \bar{A}_o(\bar{t}) + \epsilon\bar{A}_1(\bar{t}) + \ldots, \tag{24a}$$

$$\bar{a}(\bar{t};\epsilon) = \bar{a}_o(\bar{t}) + \epsilon\bar{a}_1(\bar{t}) + \ldots \tag{24b}$$

and give the following order unity approximations to Eqs. 23a and 23b:

$$\frac{d\bar{A}_o}{d\bar{t}} = g(\bar{A}_o, \bar{a}_o), \tag{25a}$$

$$\frac{d\bar{a}_o}{d\bar{t}} = 0 \tag{25b}$$

The solution to Eq. 25b is:

$$\bar{a}_o = a_* \tag{26}$$

Using this result in Eq. 25a, we obtain:

$$\frac{d\bar{A}_o}{d\bar{t}} = H(1 - \bar{A}_o) - \frac{\bar{A}_o a_*}{\bar{A}_o^2 + \gamma\bar{A}_o + \beta} \tag{27}$$

However, a_* is given by the solution to $g(A_*, a_*) = 0$, which is

$$a_* = H(1 - A_*)\,(A_*^2 + \gamma A_* + \beta)/A_* \tag{28}$$

Combining Eqs. 18, 27, and 28, we obtain:

$$\frac{d\bar{A}_o}{d\bar{t}} = -\frac{H(\bar{A}_o - A_*)^2}{\bar{A}_o^2 + \gamma\bar{A}_o + \beta}\left(\bar{A}_o - \frac{\beta}{A_*^2}\right) \tag{29}$$

as an equation for $\bar{A}_o$. The solution is implicit:

$$-\frac{\beta + \frac{\beta\gamma}{A_*^2} + \frac{2\beta}{A_*} - A_*^2}{\left(\frac{\beta}{A_*^2} - A_*\right)^2}\ln(\bar{A}_o + A_*) + \frac{A_*^2 + \gamma A_* + \beta}{\left(\frac{\beta}{A_*^2} - A_*\right)(\bar{A}_o - A_*)} + \frac{\beta + \frac{\beta\gamma}{A_*^2} + \frac{\beta^2}{A_*^4}}{\left(\frac{\beta}{A_*^2} - A_*\right)^2}\ln\left(-\bar{A}_o + \frac{\beta}{A_*^2}\right) = -H\bar{t} \tag{30}$$

To examine the possibility of matching this with the lower and upper branches of the outer solution, we require the behavior of Eq. 30 in the limits $\bar{t} \to \pm\infty$. This is:

$$\bar{t} \to \infty; \quad \bar{A}_o \sim \frac{\beta}{A_*^2} + 0(e^{-\lambda\bar{t}}), \tag{31a}$$

$$\bar{t} \to -\infty; \quad \bar{A}_o \sim A_* - \frac{A_*^2 + \gamma A_* + \beta}{H\left(\frac{\beta}{A_*^2} - A_*\right)\bar{t}}, \tag{31b}$$

in which

$$\lambda = H\left(\frac{\beta}{A_*^2} - A_*\right)^2 \Big/ \left(\beta + \frac{\beta\gamma}{A_*^2} + \frac{\beta^2}{A_*^4}\right) > 0 \tag{31c}$$

The branching-inner solution given by Eq. 30, and in its limiting form given by Eq. 31a, automatically matches with the upper branch of the outer solution. However, because of the algebraic decay with $\bar{t}$ exhibited by Eq. 31b for $\bar{t} \to -\infty$, the branching-inner solution *cannot* be matched with the lower branch of the outer solution. The implication of the failure is the existence of a second inner region over which the lower branch outer solution goes smoothly to the first branching-inner solution.

Second Transition Solution

At this stage the proper rescaling which will allow a smooth transition from the lower branch of the outer solution is unknown, so we define a new time variable given by:

$$\tilde{t} = \frac{\bar{t} - \bar{t}_o - \rho(\epsilon)}{\nu(\epsilon)} \tag{32}$$

where $\rho(\epsilon)$ is a time shift analogous to the shift $\delta(\epsilon)$ in Eq. 22 and $\nu(\epsilon)$ is the as-yet unknown rescaling. In terms of $\tilde{t}$, Eqs. 9a and 9b become:

$$\frac{\epsilon}{\nu(\epsilon)} \cdot \frac{dA}{d\tilde{t}} = H(1 - A) - \frac{Aa}{A^2 + \gamma A + \beta} \equiv g(A, a), \tag{33a}$$

$$\frac{1}{\nu(\epsilon)} \cdot \frac{da}{d\tilde{t}} = -\frac{Aa}{A^2 + \gamma A + \beta} \tag{33b}$$

We now seek a solution valid *locally*, in the vicinity of the lower branch point; the dependent variables are assumed to possess the following asymptotic representations:

$$A(\tilde{t};\, \epsilon) \sim A_* + \sigma_1(\epsilon)\,\bar{A}_1(\tilde{t}) + \ldots, \tag{34a}$$

$$a(\tilde{t};\, \epsilon) \sim a_* + \omega_1(\epsilon)\,\bar{a}_1(\tilde{t}) + \ldots \tag{34b}$$

Thus, $\bar{A}_1$, $\bar{a}_1$ represent *deviations* from the lower branch-point solution. On using these forms in Eqs. 33a and 33b, we obtain:

$$\frac{\epsilon\sigma_1}{\nu}\frac{d\bar{A}_1}{d\tilde{t}} = \omega_1\frac{\partial g_*}{\partial a}\bar{a}_1 + \frac{1}{2}\sigma_1^2\frac{\partial^2 g_*}{\partial A^2}\bar{A}_1^2 + \ldots, \tag{35a}$$

and

$$\frac{\omega_1}{\nu}\frac{d\bar{a}_1}{d\tilde{t}} = -\frac{A_* a_*}{A_*^2 + \gamma A_* + \beta} + \ldots \tag{35b}$$

where the subscript * on g indicates that the derivative is to be evaluated at the lower branch point. Although it is true that on the time-scale of $\bar{t}$ given by Eq. 22, the activity is effectively constant (Eq. 25b), it turns out that the time $\tilde{t}$ is much longer so that activity varies significantly on this scale. Thus, all three terms in Eq. 33a must balance and we have from Eq. 33b that $(\omega_1/\nu) = 0(1)$. The result is that:

$$\nu(\epsilon) = \epsilon^{2/3}, \tag{36a}$$

$$\sigma_1(\epsilon) = \epsilon^{1/3}, \tag{36b}$$

$$\omega_1(\epsilon) = \epsilon^{2/3} \tag{36c}$$

and we see that although activity changes on a much longer time-scale than concentration, it also changes on a significantly longer time-scale here than in the *first* branching inner region. With the sequence obtained, the leading-order equations are:

$$\frac{d\bar{A}_1}{d\tilde{t}} = \frac{\partial g_*}{\partial a}\bar{a}_1 + \frac{1}{2}\frac{\partial^2 g_*}{\partial A^2}\bar{A}_1^2, \tag{37a}$$

$$\frac{d\bar{a}_1}{d\tilde{t}} = -\frac{A_* a_*}{A_*^2 + \gamma A_* + \beta} \tag{37b}$$

Eq. 37b can be readily integrated to give:

$$\bar{a}_1 = -H(1 - A_*)\tilde{t} \tag{38}$$

in which we have used Eq. 16 and the constant of integration has been absorbed into the time shift $\rho(\epsilon)$. Combining Eqs. 37a and 38 gives:

$$\frac{d\bar{A}_1}{d\tilde{t}} = \frac{1}{2}\frac{\partial^2 g_*}{\partial A^2}\bar{A}_1^2 - H(1 - A_*)\frac{\partial g_*}{\partial a}\tilde{t} \tag{39}$$

This nonlinear equation for $\bar{A}_1$ possesses an exact solution which can be found as follows: define

$$T = \frac{1}{2}\frac{\partial^2 g_*}{\partial A^2}\tilde{t}, \tag{40a}$$

$$K = -\frac{H(1 - A_*)\partial g_*/\partial a}{\frac{1}{4}\left(\frac{\partial^2 g_*}{\partial A^2}\right)^2} > 0 \tag{40b}$$

Then Eq. 39 becomes:

$$\frac{d\bar{A}_1}{dT} = \bar{A}_1^2 + KT \tag{41}$$

which is of Ricatti type[a] and can be solved explicitly by means of the transformation:

$$\bar{A}_1 = -d(\ln V)/dT \tag{42}$$

If we let

$$\tau = K^{1/3}T \tag{43}$$

TABLE 1. THE FUNCTIONS $F(A)$ USED IN THE OUTER SOLUTIONS, EQS. 50 TO 52, CORRESPONDING TO VARIOUS DEACTIVATION MECHANISMS.

n	$F(A)$
	Eq. 3c Parallel Poisoning
1	$-2A + \beta \ln A - (1 + \beta + \gamma)\ln(1 - A) - \beta/A$
2	$(\beta + \gamma - 1)\ln A - (1 + \beta + \gamma)\ln(1 - A) - \beta/A - \beta/2A^2$
3	$(1 + \beta + \gamma)\ln[A/(1 - A)] - (\gamma + \beta - 1)/A - \beta/2A^2 - \beta/3A^3$
	Eq. 3d Series Poisoning
1	$2A + \beta \ln A + (3 - \beta + \gamma)\ln(1 - A) + (1 + \beta + \gamma)/(1 - A)$
2	$2\beta \ln A + 2(1 - \beta)\ln(1 - A) - \beta/A + (1 + \beta + \gamma)/(1 - A)$
3	$(\gamma + 3\beta - 1)\ln[A/(1 - A)] - 2\beta/A - \beta/2A^2 + (1 + \beta + \gamma)/(1 - A)$

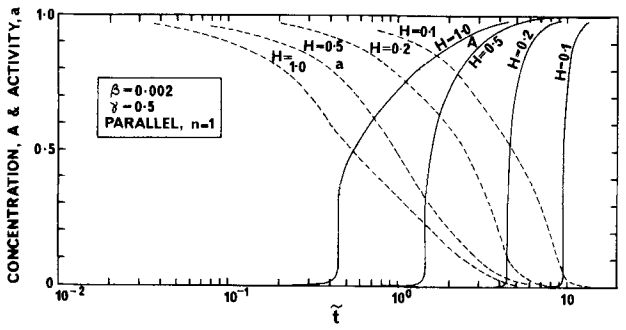

Figure 3. Effect of space velocity on time dependence of reactor performance for parallel poisoning.

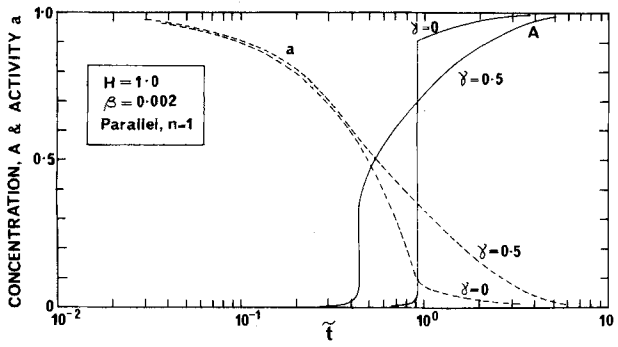

Figure 4. Effect of kinetic parameter γ on time dependence of reactor performance for parallel poisoning.

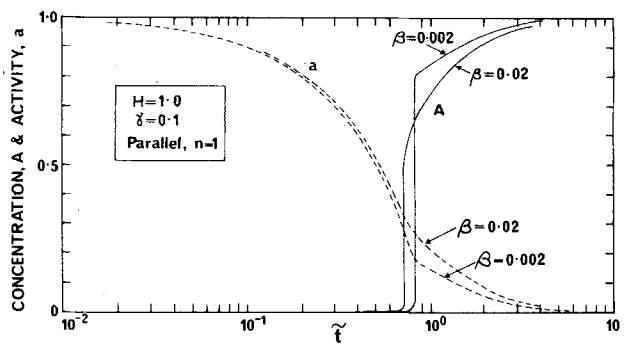

Figure 5. Effect of kinetic parameter β on time dependence of reactor performance for parallel poisoning.

then, τ is related to the original time variable $\bar{t}$ by:

$$\tau = \left[\frac{H^2 A_*^2 (1 - A_*)\,(\beta/A_*^2 - A_*)}{(A_*^2 + \gamma A_* + \beta)^2}\right]^{1/3} \bar{t} \qquad (44)$$

and Eq. 41 reduces to:

$$\frac{d^2V}{d\tau^2} + \tau V = 0 \qquad (45)$$

Eq. 45 is the well-known Airy equation; the solution can be written in terms of modified Bessel functions (Abramowitz and Stegun, 1970):

$$V = \begin{cases} c\sqrt{-\tau}\, K_{1/3}\left[\frac{2}{3}(-\tau)^{3/2}\right], & \tau < 0; \qquad (46a) \\ c\,\frac{\pi}{\sqrt{3}}\sqrt{\tau}\left[J_{1/3}\left(\frac{2}{3}\tau^{3/2}\right) + J_{-1/3}\left(\frac{2}{3}\tau^{3/2}\right)\right], & \tau > 0 \qquad (46b) \end{cases}$$

Here, c is an unknown constant which will be found by matching with the lower branch of the outer solution. From Eq. 42, we can easily obtain $\bar{\bar{A}}_1$.

For matching, we require the behavior of this second transition solution as $\bar{t} \to \pm\infty$, namely,

$\bar{t} \to -\infty$; $A \sim A_*$

$$+ c\epsilon^{1/3} \frac{H^{1/3} A_*^{1/3} (1 - A_*)^{1/6} \left(\frac{\beta}{A_*^2} - A_*\right)^{1/6}}{(A_*^2 + \gamma A_* + \beta)^{1/3}} \sqrt{-\bar{t}} + \ldots, \qquad (47a)$$

$\bar{t} \to +\infty$; $A \sim A_*$

$$+ c\epsilon^{1/3} \frac{(A_*^2 + \gamma A_* + \beta)^{2/3}}{H^{2/3} A_*^{2/3} (1 - A_*)^{1/3} \left(\frac{\beta}{A_*^2} - A_*\right)^{1/3}} \cdot \frac{1}{\bar{t}} + \ldots \qquad (47b)$$

Eq. 47a can be made to match with the lower branch of the outer solution (Eq. 10b) as $(\bar{t} - \bar{t}_0) \to 0-$ if we choose

$$c = -\left[\frac{(A_*^2 + \gamma A_* + \beta)\,(1 - A_*)A_*^2}{H(\beta/A_*^2 - A_*)^2}\right]^{1/3} \qquad (48)$$

With this value of c, Eq. 47b is:

$$A \sim A_* - \epsilon^{1/3} \frac{A_*^2 + \gamma A_* + \beta}{H(\beta/A_*^2 - A_*)\bar{t}} \qquad (49)$$

and this automatically matches with the first branching-inner expansion as $\bar{t} \to -\infty$ (Eq. 31b).

This completes the solution to the reactor failure problem to leading order. In principle, one could write down the composite expansion which would contain all the information of the inner, lower branch outer, first branching inner, second branching inner, and upper branch outer expansions. However, some of these solutions have been able to be given only implicitly, so an explicit composite solution cannot be presented.

OTHER DEACTIVATION RATE FORMS

In previous sections, we have analyzed in some detail the way in which one can determine the branching time and the way in

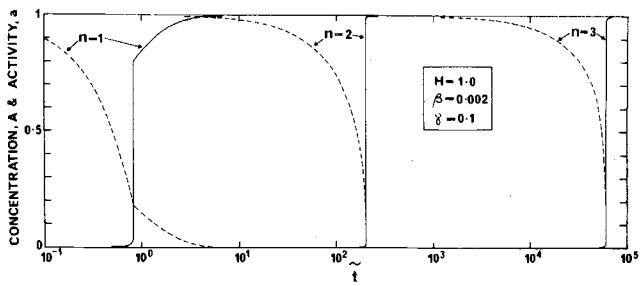

Figure 6. Effect of various parallel mechanisms on reactor performance, ——, a; ——, A.

[*] That such transition regions are governed by a Ricatti equation seems typical. See, for example, Haberman (1979) for a discussion of slow passage through critical.

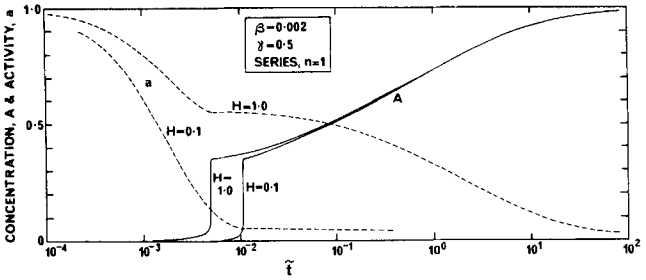

Figure 7. Effect of space velocity on time dependence of reactor performance for series poisoning.

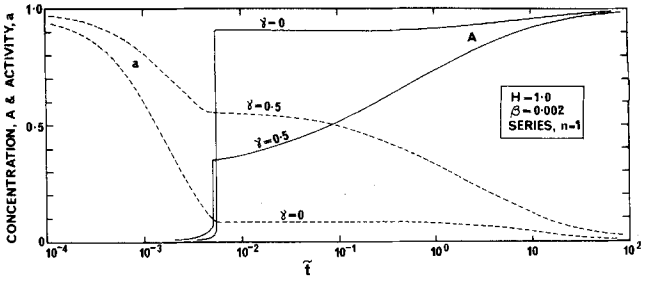

Figure 8. Effect of kinetic parameter γ on time dependence of reactor performance for series poisoning.

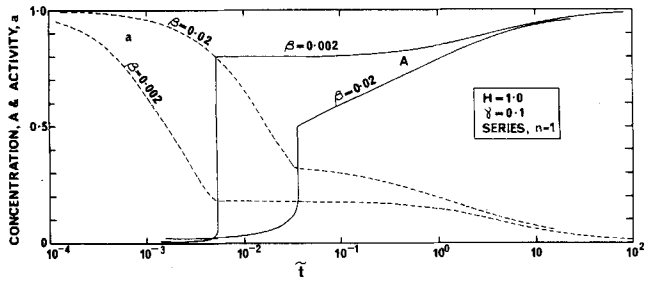

Figure 9. Effect of kinetic parameter β on time dependence of reactor performance for series poisoning.

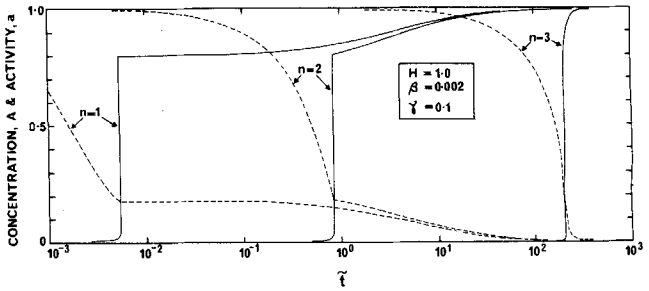

Figure 10. Effect of various series mechanisms on reactor performance, ---, a; ——, A.

which the reactor makes a smooth transition from one branch of the solution to the other. This section presents the key results for other mechanisms given by Eqs. 1c and 1d for parallel and series deactivation, respectively, when the exponent n takes on the integer values {1, 2, 3}.

We find that:

$$a = H(1 - A)\,(A^2 + \gamma A + \beta)/A \tag{50}$$

and A is given implicitly by:

$$F(A) - F(A^+) = \tilde{t}; \quad \tilde{t} < \tilde{t}_o, \tag{51a}$$

$$F(A) - F(A^*) = \tilde{t} - \tilde{t}_o; \quad \tilde{t} > \tilde{t}_o \tag{51b}$$

where $F(A)$ is given in Table 1 for the various deactivation mechanisms. The branching time $\tilde{t}_o$ is found from

$$\tilde{t}_o = F(A_*) - F(A^+) \tag{52}$$

DISCUSSION

It will be appreciated that because of the large number of parameters involved, we are able to give only representative samples of the jump phenomenon. Typical plots showing the effect of various parameters on the time dependence of reactant concentration and activity are given in Figures 3 to 6 for parallel deactivation and Figures 7 to 10 for a series mechanism.

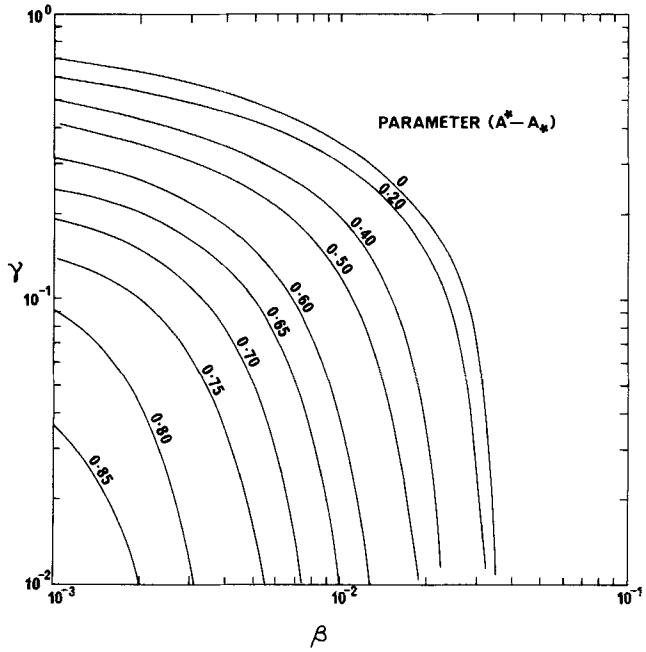

Figure 11. Magnitude of concentration jump as a function of kinetic parameters β and γ.

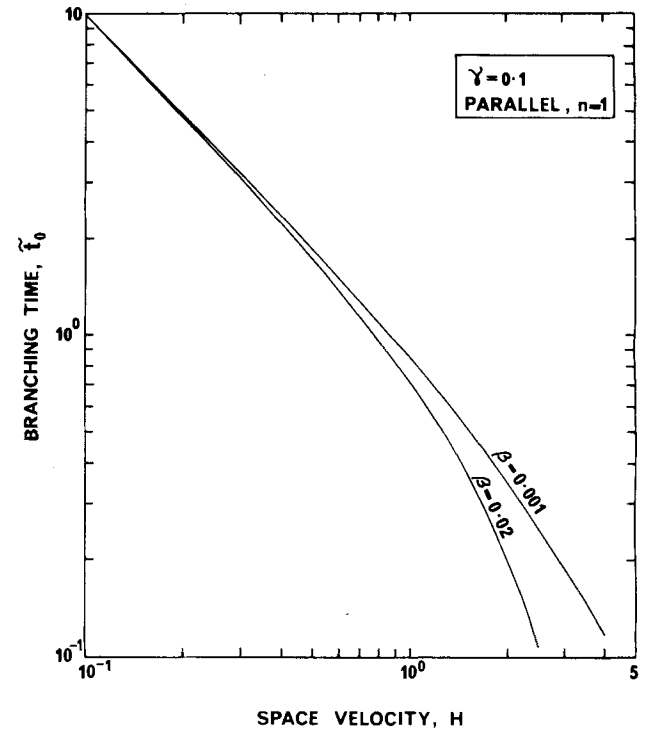

Figure 12. Effect of β on branching time for parallel deactivation.

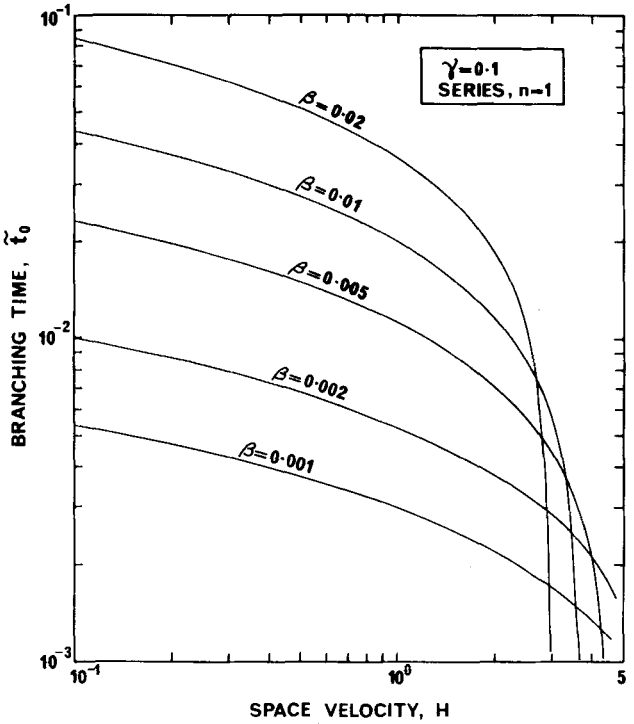

Figure 13. Effect of β on branching time for series deactivation.

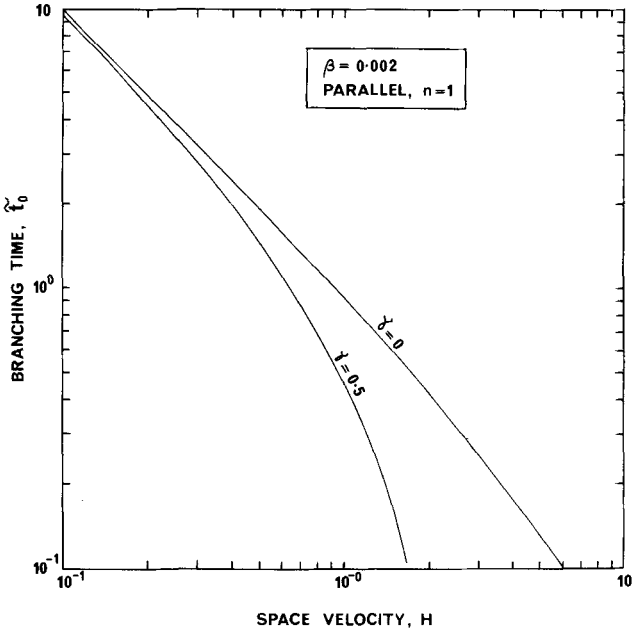

Figure 14. Effect of γ on branching time for parallel deactivation.

As the space velocity through the reactor increases, reactant concentration is maintained at somewhat higher levels so that for parallel poisoning (Figure 3) activity begins to decline sooner. On the other hand, product concentration is maintained at lower levels so that for series (product) poisoning (Figure 7) the fall in activity is delayed. Nevertheless, an increase in space velocity results in earlier occurrence of the jump across pseudo-steady states in both cases; the effect is much more pronounced for reactant poisoning. It is noteworthy that at high space velocities the loss in performance takes place when the catalyst still retains significant activity. Thus, it is in reactors operating at high throughput that one might expect to see an early and disastrous loss in performance.

Comparing Figures 4 and 8, it can be seen that an increase in the kinetic parameter γ causes an earlier loss in performance for reactant poisoning but hardly affects the jump time at all for series poisoning. The reverse is true for an increase in β (Figures 5 and 9) which causes only a slightly earlier performance loss for parallel deactivation but substantially delays the time of reactor failure when the product is responsible for poisoning.

When the jump occurs, the concentration of product experiences a sudden decrease. As a result, catalyst decay is nearly arrested (at its value at the time of the jump) for series deactivation. But the rate of activity loss decreases somewhat for parallel poisoning too, despite the fact that the poison concentration has increased. This is because of the form of the rate expression for deactivation; when A increases, the factor $A/(A^2 + \gamma A + \beta)$ *decreases* in Eq. 1c and da/dt drops. (See also Figure 1.)

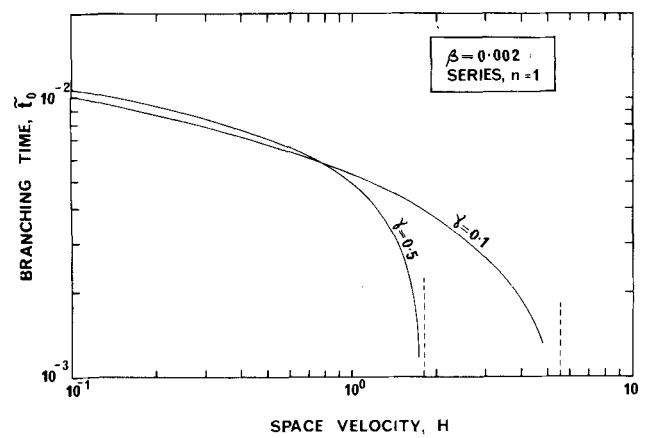

Figure 15. Effect of γ on branching time for series deactivation.

The effect of the details of the deactivation mechanism (n = 1, 2, 3) can be seen in Figures 6 and 10 for parallel and series poisoning, respectively. As the mechanism becomes more complex (n increases) the time at which reactor failure occurs is delayed by factors of the order of 100, but it is made more severe when it does occur. For the parameter values indicated, however, the catalyst is largely deactivated by the time the jump takes place. Finally, when Figures 3 to 6 are compared with their counterparts for series deactivation (Figures 7 to 10), it can be seen that reactor failure occurs sooner by a factor of hundreds for series poisoning than for a parallel mechanism.

It is interesting to note that the magnitude of the jump, $(A^* - A_*)$, is quite *independent* of both the poisoning mechanism and the reactor space velocity. As shown in Figure 11, it depends solely on the kinetic parameters β and γ. The contour marked $A^* - A_* = 0$ separates the regions of unique and multiple steady states. The smaller the values of β and γ, the larger will be the concentration jump for a deactivating catalyst.

Figures 12 to 15 deal with the effect of reactor space velocity on the branching time for various values of β and γ. These Figures reinforce our earlier comments that a high throughput results in very early loss of performance. Increasing β causes only slightly earlier failure for a given space velocity under a parallel mechanism, but the jump time is extremely sensitive to β for a series mechanism (Figures 12 and 13). Furthermore, for series poisoning increasing β can either accelerate the time of failure, or delay it, depending on the throughput at which the reactor is operating (Figure 13). As shown in Figure 15, a similar remark can be applied to the effect of γ for series poisoning, although at low space velocities this parameter barely affects the branching time. The fact that these curves asymptote to particular values of H merely indicates that satisfactory operation cannot be established above a certain space velocity whose value depends on the kinetic parameters and the type and complexity of the deactivation mechanism.

The way in which the reactor moves across the jump in steady states is exemplified in Figure 16; the parameter values are H = 1.0, β = 0.002, γ = 0.1, and ϵ = 0.001. The transition curve is a composite of the four asymptotic expansions valid in the pre-branching, branching, and postbranching periods. It should be noted that the time variable is $\bar{t}$, since it is only on such a

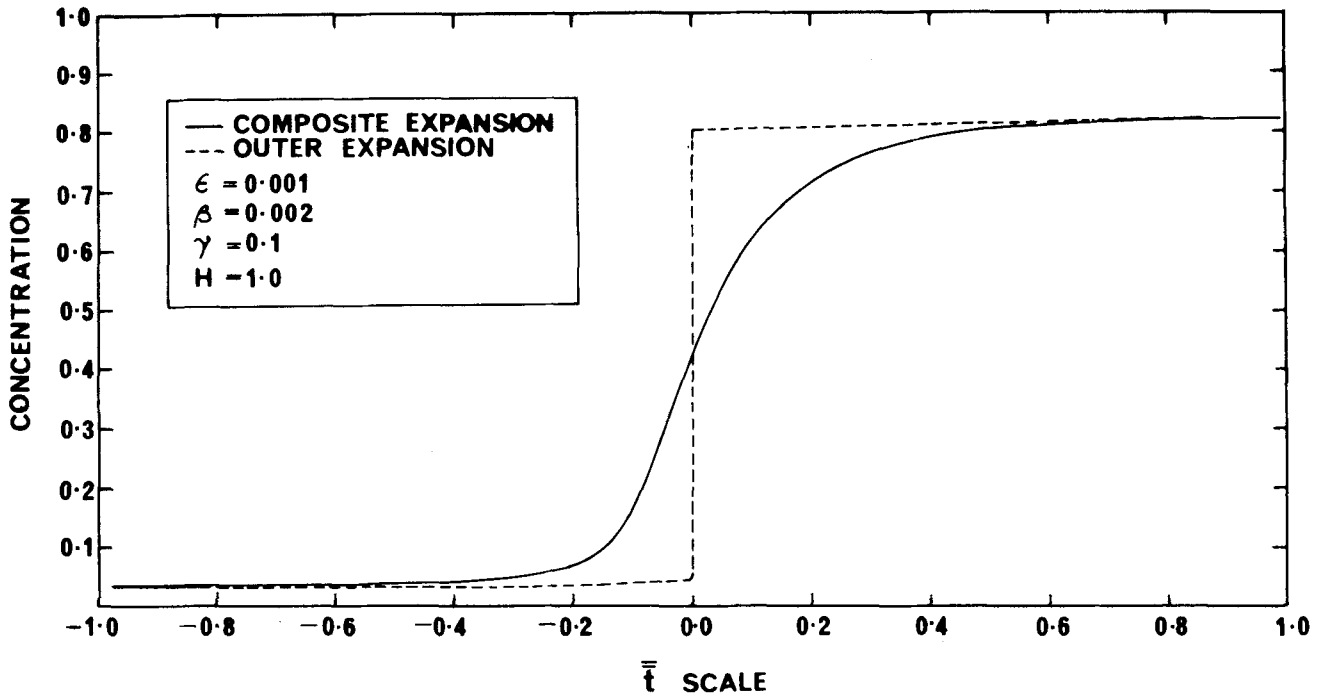

Figure 16. Detailed structure of the jump.

time-scale that the details of the transition become visible. The point $\bar{t} = 0$ corresponds exactly to the branching time $\tilde{t}_o$. It can be seen that as time approaches $\tilde{t}_o$, the reactant concentration begins to rise sharply, but that it takes a considerable time for it to reach its new pseudo-steady level. The transition is asymmetric about the branching time.

NOTATION

a = catalyst activity
a_* = catalyst activity at branching time $\tilde{t}_o$
a_i = defined in Eq. 3b
$\tilde{a}_i$ = defined in Eq. 8b
$\bar{a}_i$ = defined in Eq. 24b
$\bar{\bar{a}}_i$ = defined in Eq. 34b
A = nondimensional reactant concentration (C_A/C_{Ao})
A^+ = first quasilevel of A, smallest root of Eq. 5c
A_* = concentration of A at lower branch point
A^* = concentration of A at start of upper branch
$A^\sharp$ = concentration of A at upper branch point
A_i = defined in Eq. 3a
$\tilde{A}_i$ = defined in Eq. 8a
$\bar{A}_i$ = defined in Eq. 24a
$\bar{\bar{A}}_i$ = defined in Eq. 34a
B = nondimensional product concentration (C_B/C_{Ao})
c = constant defined in Eq. 48
C_A = dimensional reactant concentration in bulk
C_{Ao} = dimensional reactant concentration in feed
C_B = dimensional product concentration in bulk
F = feed rate to reactor
$F(A)$ = function given in Table 1
$g(A, a)$ = function defined in Eq. 2a
H = nondimensional space velocity ($= FC_{Ao}^2/kV$)
k = rate constant for the main reaction
k_d = deactivation rate constant
K = kinetic constant, or function defined in Eq. 40b
K_s = kinetic constant
n = exponent in Eqs. 1a to 1f
R = reaction or deactivation rate
t = nondimensional time ($= kt'/C_{Ao}^2$)
t' = dimensional time
$\tilde{t}$ = long time variable defined in Eq. 6
$\tilde{t}_o$ = branching time
$\bar{t}$ = time defined in Eq. 22
$\bar{\bar{t}}$ = time defined in Eq. 32
T = time defined in Eq. 40a
V = function defined in Eq. 42, or reactor volume

Greek Letters

β = kinetic constant ($= K/C_{Ao}^2$)
γ = kinetic constant ($= K_s/C_{Ao}$)
$\delta(\epsilon)$ = time shift in Eq. 22
ϵ = nondimensional deactivation rate constant ($= k_d C_{Ao}^n/k$)
λ = exponent defined in Eq. 31c
$\nu(\epsilon)$ = time scale used in Eq. 32
$\rho(\epsilon)$ = time shift in Eq. 32
$\sigma_1(\epsilon)$ = coefficient in Eq. 34a
τ = time defined in Eq. 43
ω = deviation variable ($= A - \tilde{A}_o$)
$\omega_1(\epsilon)$ = coefficient in Eq. 34b

LITERATURE CITED

Abramowitz, M., and I. Stegun, *Handbook of Mathematical Functions*, Dover Publications, New York (1970).

Bruns, D. D., J. E. Bailey, and D. Luss, "Steady State Multiplicity and Stability of Enzymatic Reaction Systems," *Biotech. Bioeng.*, **15**, 1131 (1973).

DeVera, A. L., and A. Varma, "Substrate-Inhibited Enzyme Reaction in a Tubular Reactor with Axial Dispersion," *Chem. Eng. Sci.*, **34**, 275 (1979).

Do, D. D., and R. H. Weiland, "Catalyst Deactivation in an Isothermal CSTR with First-Order Chemical Kinetics," *Chem. Eng. J.* (1979a).

Do, D. D., and R. H. Weiland, "Catalyst Deactivation in an Isothermal CSTR with N-th Order and Michaelis-Menten Kinetics," *Chem. Eng. J.* (1979b).

Do, D. D., and R. H. Weiland, "Consistency between Rate Expressions for Enzyme Reactions and Deactivation," *Biotech. Bioeng.*, **22**, 1087 (1980a).

Do, D. D., and R. H. Weiland, "Substrate-Inhibited Kinetics with Catalyst Deactivation in an Isothermal CSTR—Unique Pseudosteady State," *AIChE J.* **26**, 948 (1980).

Gavalas, G. R., *Nonlinear Differential Equations of Chemically Reacting Systems*, Springer-Verlag, Berlin, West Germany (1968).

Haberman, R., "Slowly Varying Jump and Transition Phenomena Associated with Algebraic Bifurcation Problems," *SIAM J. Appl. Math.*, 37, 69 (1979).

Manuscript received October 1, 1979; revision received April 28 and accepted May 1, 1980.